



Effectiveness of Micro-Blowing Technique in Adverse Pressure Gradients

Gerard E. Welch and Louis M. Larosiliere
U.S. Army Research Laboratory, Glenn Research Center, Cleveland, Ohio

Danny P. Hwang and Jerry R. Wood
Glenn Research Center, Cleveland, Ohio

DISTRIBUTION STATEMENT A
Approved for Public Release
Distribution Unlimited

DTIC QUALITY INSPECTED 4

20010105 015

The NASA STI Program Office . . . in Profile

Since its founding, NASA has been dedicated to the advancement of aeronautics and space science. The NASA Scientific and Technical Information (STI) Program Office plays a key part in helping NASA maintain this important role.

The NASA STI Program Office is operated by Langley Research Center, the Lead Center for NASA's scientific and technical information. The NASA STI Program Office provides access to the NASA STI Database, the largest collection of aeronautical and space science STI in the world. The Program Office is also NASA's institutional mechanism for disseminating the results of its research and development activities. These results are published by NASA in the NASA STI Report Series, which includes the following report types:

- **TECHNICAL PUBLICATION.** Reports of completed research or a major significant phase of research that present the results of NASA programs and include extensive data or theoretical analysis. Includes compilations of significant scientific and technical data and information deemed to be of continuing reference value. NASA's counterpart of peer-reviewed formal professional papers but has less stringent limitations on manuscript length and extent of graphic presentations.
- **TECHNICAL MEMORANDUM.** Scientific and technical findings that are preliminary or of specialized interest, e.g., quick release reports, working papers, and bibliographies that contain minimal annotation. Does not contain extensive analysis.
- **CONTRACTOR REPORT.** Scientific and technical findings by NASA-sponsored contractors and grantees.

- **CONFERENCE PUBLICATION.** Collected papers from scientific and technical conferences, symposia, seminars, or other meetings sponsored or cosponsored by NASA.
- **SPECIAL PUBLICATION.** Scientific, technical, or historical information from NASA programs, projects, and missions, often concerned with subjects having substantial public interest.
- **TECHNICAL TRANSLATION.** English-language translations of foreign scientific and technical material pertinent to NASA's mission.

Specialized services that complement the STI Program Office's diverse offerings include creating custom thesauri, building customized data bases, organizing and publishing research results . . . even providing videos.

For more information about the NASA STI Program Office, see the following:

- Access the NASA STI Program Home Page at <http://www.sti.nasa.gov>
- E-mail your question via the Internet to help@sti.nasa.gov
- Fax your question to the NASA Access Help Desk at 301-621-0134
- Telephone the NASA Access Help Desk at 301-621-0390
- Write to:
NASA Access Help Desk
NASA Center for AeroSpace Information
7121 Standard Drive
Hanover, MD 21076

NASA/TM—2001-210690

ARL-TR-2382
AIAA-2001-1012



Effectiveness of Micro-Blowing Technique in Adverse Pressure Gradients

Gerard E. Welch and Louis M. Larosiliere
U.S. Army Research Laboratory, Glenn Research Center, Cleveland, Ohio

Danny P. Hwang and Jerry R. Wood
Glenn Research Center, Cleveland, Ohio

Prepared for the
39th Aerospace Sciences Meeting and Exhibit
sponsored by the American Institute of Aeronautics and Astronautics
Reno, Nevada, January 8-11, 2001

National Aeronautics and
Space Administration

Glenn Research Center

January 2001

Acknowledgments

The authors thank Dr. Eric R. McFarland of NASA Glenn Research Center for supporting this work with panel code calculations, Mr. Charles A. Herrmann for engineering design work, and Ms. Gwynn A. Severt, Mr. Carlos R. Gomez, and Mr. Scott R. Panko for facility set-up, operation, and testing.

Available from

NASA Center for Aerospace Information
7121 Standard Drive
Hanover, MD 21076
Price Code: A03

National Technical Information Service
5285 Port Royal Road
Springfield, VA 22100
Price Code: A03

Available electronically at <http://gltrs.grc.nasa.gov/GLTRS>

Effectiveness of Micro-Blowing Technique in Adverse Pressure Gradients

Gerard E. Welch* and Louis M. Larosiliere
U.S. Army Research Laboratory at Lewis Field

Danny P. Hwang* and Jerry R. Wood
NASA John H. Glenn Research Center at Lewis Field

Abstract

The impact of the micro-blowing technique (MBT) on the skin friction and total drag of a strut in a turbulent, strong adverse-pressure-gradient flow is assessed experimentally over a range of subsonic Mach numbers ($0.3 < M < 0.7$) and reduced blowing fractions ($0 \leq 2F/C_{f,0} \leq 1.75$). The MBT-treated strut is situated along the centerline of a symmetric 2-D diffuser with a static pressure rise coefficient of 0.6. In agreement with presented theory and earlier experiments in zero-pressure-gradient flows, the effusion of blowing air reduces skin friction significantly (e.g., by 60% at reduced blowing fractions near 1.75). The total drag of the treated strut with blowing is significantly lower than that of the treated strut in the limit of zero-blowing; further, the total drag is reduced below that of the baseline (solid-plate) strut, provided that the reduced blowing fractions are sufficiently high. The micro-blowing air is, however, deficient in streamwise momentum and the blowing leads to increased boundary-layer and wake thicknesses and shape factors. Diffuser performance metrics and wake surveys are used to discuss the impact of various levels of micro-blowing on the aerodynamic blockage and loss.

Nomenclature

A	= area
c_f	= local skin friction coefficient
C_f	= integral skin friction coefficient
C_D	= total drag coefficient
c_p	= $(p_2 - p_1)/(p_{0,1} - p_1)$, diffuser static pressure rise coefficient
c_p^i	= ideal static pressure rise coefficient
C_p	= integral pressure force coefficient
δ_0	= boundary layer height
δ_1	= displacement thickness
δ_2	= momentum thickness
f	= Blasius function
F	= $(\rho v)_B / (\rho u)_\infty$, blowing fraction
F^+	= $2F/C_{f,0}$, reduced blowing fraction
G	= blowing to freestream mass flow rate ratio
H	= δ_1/δ_2 , shape factor
L	= chord of strut

\dot{m}	= mass flow rate
M	= Mach number
\bar{p}	= area-averaged pressure
\tilde{p}	= mass-averaged pressure
$Re_{L,0}$	= Reynolds number based on strut chord and inlet total conditions
Re_x	= Reynolds numbers based on axial position and freestream conditions
T	= temperature
u	= axial velocity component
v	= transverse velocity component
W	= width of strut
x	= axial direction
y	= transverse direction
γ	= ratio of specific heats
η	= $(y/x)\sqrt{Re_x}$, Blasius similarity parameter
η_D	= diffuser effectiveness (Eqn. 2).
ρ	= mass density
ω	= loss coefficient

Subscripts

0	= stagnation condition
1	= diffuser inlet (throat)
2	= diffuser exit
B	= blowing air
S	= solid plate (baseline) value
∞	= freestream value
*	= variable normalized by zero-blowing value

*Senior member of AIAA.

Copyright © 2001 by the American Institute of Aeronautics and Astronautics, Inc. No copyright is asserted in the United States under Title 17, U.S. Code. The U.S. Government has a royalty-free license to exercise all rights under the copyright claimed herein for Governmental Purposes. All other rights are reserved by the copyright owner.

Introduction

The micro-blowing technique (MBT) is a passive method for reducing the skin-friction component of total drag in which a small investment of air is effused through holes of specific shape and distributed porosity. The "micro" refers both to the minimal investment of blowing air required—typical blowing fractions, F , are on the order of 0.1%—and to the small size of the blowing holes relative to the local momentum thickness. Hwang demonstrated that MBT can be used to reduce the skin friction of a flat-plate in a subsonic, zero-pressure-gradient flow by as much as 60%.¹ Significant reductions were obtained throughout a wide range of Reynolds and Mach numbers. Similar reductions in the skin friction levels of an MBT-treated nacelle were reported by Tillman in regions of mild adverse pressure gradient.²

The micro-blowing technique is described in detail elsewhere.¹ The blowing air is typically effused normal to the treated surface. Evidently the addition of this air, which is deficient in streamwise momentum, increases aerodynamic blockage. In an external flow (e.g., a wing) this leads to increased pressure drag while in an internal flow (e.g., a diffuser) the pressure recovery is decreased. Even so, Hwang and Biesiadny demonstrated that MBT could be applied to reduce the total drag of an uncambered strut in a zero-pressure-gradient test section by 2% at blowing fractions near 0.2%.³ Their experiment demonstrated that the decrease in the skin-friction component associated with micro-blowing could in some circumstances win out over the inevitable increase in pressure drag penalty.

The work described herein is motivated by the potential application of the micro-blowing technique to reduce the total drag of surfaces in external flows and the loss production in the boundary layers of internal flows. The flow fields considered are subsonic and turbulent. The primary objective is to assess the impact of micro-blowing on skin friction and total drag in strong adverse pressure gradients typical of highly loaded airfoils and diffusers. A second related objective is to investigate the viability of using micro-blowing to increase the effectiveness of diffusing sections.

An analytical description of flow over transpired surfaces is first used to discuss the impact of transpiration on skin friction, entropy production, boundary layer stability, and aerodynamic blockage. An experiment to assess the benefits of micro-blowing in adverse-pressure-gradient flows is then described. The results from this experiment are presented, followed by related discussion. The final section summarizes the paper.

Theory

The primary purpose of the present investigation is to ascertain the efficacy of micro-blowing to reduce skin friction and total drag in subsonic, turbulent flows in adverse pressure gradients. It is deemed valuable, however, to review the expected impact of transpiration on boundary layers in general (cf. Schlichting⁴). Consider a laminar flow over a "micro" transpired surface in a zero pressure gradient. The Blasius equation $f''' = -\frac{1}{2}f \cdot f''$ is solved with the boundary conditions that enforce zero axial velocity at the surface, $f'(0) = 0$, transpiration (blowing or suction) at the surface, $f(0) = -2 \cdot F \cdot \sqrt{\text{Re}_x}$, and matching at the freestream, $f'(\infty) = 1$. The Blasius function, $f(\eta)$, was found using a Runge-Kutta integration scheme (after White⁵) along with an iterative search for $f''(0)$. The velocity profiles for various transpiration factors are shown in figures 1 and 2 and relevant normalized boundary layer parameters are shown in Table 1. It is evident from the axial velocity profiles in Fig. 1 that blowing increases the boundary layer thickness, decreases the wall shear stress, and destabilizes the flow. Suction has the opposite impact. Transpiration impacts both the magnitude and shape of the transverse velocity component as shown in Fig. 2.

"Micro" or "Macro". As seen in the axial velocity profiles (Fig. 1) and by the normalized boundary layer thicknesses, δ_1^* and δ_2^* (Table 1), the seemingly small amounts of transpiration change the boundary-layer thicknesses substantially. Indeed, consistent with predictions from the integral boundary-layer theory for zero-pressure-gradient flows with and without transpiration, $\delta_2^* \approx C_f / C_{f,0} + 2F / C_{f,0}$. Based on this view of the impact of transpiration on momentum thickness, the magnitude of the transpiration fractions should be interpreted relative to the magnitude of the skin friction coefficient in the zero-blowing limit; hence, the reduced blowing fraction is defined as $F^+ \equiv 2F / C_{f,0}$ (cf. Hefner and Bushnell⁶). The "micro" transpiration levels considered in these examples are in reality "macro" in terms of impact on the boundary layer.

Skin friction reduction and entropy production. By considering Table 1, it is evident that blowing reduces skin friction (e.g., $C_f^* = 0.47$ @ $F^+ = 0.8$) substantially while suction increases skin friction ($C_f^* = 1.60$ @ $F^+ = -0.8$). The impact of the transpiration on skin friction is in agreement with the Falkner-Skan solutions for transpired flows by Nickel (as reported in Ref. 4). The micro-blowing reduces loss levels significantly (e.g., $\omega^* = 0.61$ @ $F^+ = 0.8$) as well, while suction strongly increases the loss levels (e.g., $\omega^* = 1.55$ @ $F^+ = -0.8$).

Note however that the effused air is necessarily of low total pressure (*i.e.*, equal to the freestream static) and therefore, although the boundary-layer entropy production is reduced, the mass-averaged total pressure of the aggregate boundary-layer flow might in some cases be lower than that of an untreated boundary layer.

Stability. The blowing destabilizes the flow field as reflected in the increased shape factor relative to the zero-blowing case while suction stabilizes the flow. Even at "micro"-blowing levels, the boundary layers are substantially more susceptible to separate than those with zero or negative transpiration (suction).

Aerodynamic blockage. In the case of an external flow, for example a wing, the increased displacement and momentum thicknesses and hence the wake thickness associated with the injection of blowing air implies increased pressure drag. The impact of the blowing on total drag will therefore depend on the trade between the decreased skin friction drag and the increased pressure drag, the impact of the latter which is scaled by the thickness-to-chord ratio. Analogously, in a diffuser, the increased displacement thickness and momentum thickness associated with micro-blowing will effectively decrease the aerodynamic area available for diffusion. The diffuser pressure rise will be dependent on balance between this increased aerodynamic blockage and decreased loss production in the boundary layers.

As seen above, normalized transpiration levels of order unity lead to significant changes in the near-wall flow. Blowing should reduce skin friction and boundary layer loss production substantially; however, the boundary layer is destabilized and aerodynamic blockage is increased. It is anticipated that the same trends hold for the turbulent flows in the adverse pressure gradients of the experiment described below.

Experiment Description

Wind Tunnel

The wind tunnel described in Ref. 3 was modified to investigate the benefits offered by MBT in strong adverse-pressure-gradients. New sidewalls were designed so that an adverse pressure gradient would be established along an uncambered strut situated along the tunnel centerline. The profiling of the sidewalls of the 2-D diffuser is shown in Fig. 3. The diffuser static pressure rise coefficient, c_p , measured from throat to exit, is approximately 0.6. Static taps are located at mid-height along the sidewalls and along the center of the top wall. Five static taps are aligned along the top wall at the $x = 33$ " location, approximately 6" (1/3-chord, 7-thicknesses) downstream of the strut trailing edge. A traversing total pressure probe is used to obtain

wake surveys between $y = -2$ " and $y = 2$ " at this same $x = 33$ " position. The measured static pressure distribution at mid-height along one of the sidewalls is shown in Fig. 4 (baseline case).

Model Description

The uncambered strut is located at in the center of the diffuser as shown in Fig. 3. The elliptical nose is situated near the diffuser throat and the wedge shaped tail is situated near the diffuser exit. The strut is mounted on an axial force balance located beneath the tunnel floor. The strut has two internal chambers, one forward and one in the tail, and is 18" long, 5.4" high, and 0.8" thick. Airlines route air to (or from) the fore and aft chambers from air supplies (or vacuum exhaust). In the tests reported herein, the aft chamber is sealed by solid plates and isolated from the forward chamber. Both sides of the forward portion of the strut are treated with a set of flush-mounted MBT plates (4.87" high and 9.87" long). Blowing is applied over $2/18 \leq x/L \leq 12/18$. The PN23 plates of Hwang's earlier experiment¹ were tested in the present work. As in earlier experiments, low permeability polyethylene backing was used to promote pressure equalization in the chambers and uniform blowing fraction delivery. The leading edges of the plates were 2.0" downstream from the leading edge of the strut. A trip strip is used to initiate a turbulent boundary layer 1" upstream of the MBT plate. To obtain the baseline (solid-plate) measurements, two interchangeable solid plates replace the two MBT plates over the fore chamber.

Force Balance Measurement and Pressure Calibration

The force balance provides a direct measurement of the reaction to the aerodynamic forces acting on the strut, the sub-platform mounting stand, and the balance surfaces. Because the strut sits in a diffuser, the net force is positive—that is, thrust rather than drag. This is counter-intuitive at first and indeed means that if the strut broke free it would initially move upstream, against the flow! The thrust is due to the pressure loading impressed on the strut by the diffusing flow—the nose is in the low-pressure region at the throat and the tail is in the higher-pressure region near the end of the diffusing section. The force balance measurement strategy therefore accommodates both axial thrust and drag measurements. The balance was preloaded using springs so that thrust forces would register more positive while drag forces would register less positive. It was also necessary to tare out the pressure loading on the mounting stand to account for the sub-platform pressure loading. A calibration curve related pressure measurements from two sidewall static taps located near the leading and trailing edge of the strut to the forces on the mounting stand. During this calibration, the strut was mounted to the tunnel ceiling so as to

preserve the pressure gradient impressed by the strut on the mounting plate. The force on the mounting plate and the two static pressures were then measured at various Mach numbers. The resulting linear calibration curve is shown in Fig. 5. At any run condition, the measured static pressures are used to infer the tare force associated with the pressure loading on the mounting plate.

Test Results

The inlet stagnation pressure was fixed at 7.5 psia for the results presented herein and the total temperature of the tunnel and blowing air was near 530 R. The chord Reynolds number, $Re_{L,0}$, based on the inlet total conditions was approximately five million (5.2 E6). The turbulence intensity of the tunnel was not measured but is known from previous testing to be relatively high and to depend upon the load demand in adjacent test facilities. Again, the trip strip was used to initiate a turbulent boundary layer upstream of the leading edge of the MBT plates. Tunnel back pressure was varied to set throat Mach numbers in increments of 0.1 between $0.3 < M < 0.7$. The blowing fraction was varied between $0 < F < 0.002$ in increments of 0.0005. The corresponding ratios of bleed mass flow rate to through flow mass flow rate were as high as $G = 0.5\%$. The maximum blowing fraction was set by the flow capacity of the blowing air supply system.

In a typical series of tests, solid plates were first installed and baseline values were established for the various throat Mach numbers. The MBT plates were then installed and tests were conducted over the same range of Mach numbers at the various blowing fractions. A force balance calibration was carried out each time the plates were changed, for example, from the MBT to the solid plates. There was significant scatter in the force balance measurements before and after plate change-out whereas for a given plate configuration (solid or MBT) the force measurements repeated through repeated sweeps of Mach number and blowing fractions with negligible scatter or hysteresis. This points to a limit in the accuracy of the force balance measurement system at the small load levels established on the strut associated with plate change-out. Each case was therefore run several times and the mean value and some sense of the deviation was obtained. Disparity in force balance measurements were as large as 20% at the low Mach numbers at which the net forces are smallest.

Skin friction reduction

The difference between the integral skin friction coefficients of the MBT and solid-plate tests at fixed Mach numbers are related by

$$\Delta C_f = \Delta C_D + \frac{W}{2L} \Delta C_p \quad (1)$$

The integral pressure coefficients are obtained by using static pressure data from sidewall taps in the vicinity of the tail of the strut. The difference between the integral pressure coefficients of two tests at the fixed Mach number is essentially equivalent to the difference between the static pressure rise coefficients (*i.e.*, $\Delta C_p \approx \Delta c_p$). The drag coefficients are obtained directly from the force balance measurements with the pressure tare force correction (see Fig. 5). The ΔC_f values calculated using Eqn. 1 were then doubled to normalize to the MBT plates that cover only half the strut planform area; that is, the changes in C_f are credited to reductions in the shear force at the MBT plates, seemingly a very reasonable assumption. To contextualize the level of the calculated changes in skin friction coefficient, data from the solid-plate experiments of Ref. 1 were used to set the skin friction coefficient of the baseline (solid-plate) to 0.0039.

The reduced skin friction data (symbols) are shown in Fig. 6; evidently, these data compare well with the bounds of Rubesin's data (dashed curves) as reported by Hefner and Bushnell.⁶ $C_{f,0}$ denotes the skin friction coefficient of the MBT-treated strut in the limit of zero blowing fraction. Consistent with findings in Ref. 1, the experimentally determined $C_{f,0}$ is essentially equivalent to $C_{f,s}$ (*i.e.*, 0.0039). This highlights the efficiency of the MBT plates and means that the skin friction reduction with blowing relative to the baseline (solid-plate), $C_f/C_{f,s}$, is equivalent to the skin friction reduction relative to the zero-blowing limit, $C_f/C_{f,0}$. Note that the scaling suggested by integral boundary layer theory described earlier collapses the data. Interestingly, by multiplying the reduced blowing fraction by a factor of two (solid curve), the analytical theory can be used as an accurate basis for the data. As found for zero- or mildly adverse-pressure-gradient flows,^{1,2,6} the micro-blowing substantially reduces skin friction in this strong adverse-pressure-gradient flow.

Diffuser pressure coefficient and effectiveness

The increased aerodynamic blockage associated with the effusion of micro-blowing air evidently leads to reduced diffuser c_p as shown in Fig. 7. Indeed, to first order, the c_p of the diffuser is reduced with blowing fraction ($c_p \approx c_p' - \omega - G$). The benefit of reduced viscous dissipation (or loss) in the boundary layers has evidently fallen below the detrimental impact of increased blockage. A comparison of the axial pressure distributions in Fig. 4 shows evidence of the loss of effective aerodynamic area available for diffusion with

increased blowing fraction. The diffuser effectiveness (cf. Shapiro⁷) provides an indication of the thermodynamic efficiency of the diffusion process and is calculated using the formula

$$\eta_D = \frac{1 + \frac{\gamma-1}{2} M_2^2}{\frac{\gamma-1}{2} (M_1^2 - M_2^2)} \left(\frac{1+G}{1+G \cdot T_b/T_{01}} \left[\frac{P_2}{P_1} \right]^{\gamma/(\gamma-1)} - 1 \right) \quad (2)$$

where

$$(\gamma-1)M_2^2 = \left(\frac{1 + 2(\gamma-1)(1+G)(1+G \cdot T_b/T_{01})}{(A_1 P_1 / (A_2 P_2))^2 (M_1^2 + \frac{\gamma-1}{2} M_1^4)} \right)^{1/2} - 1 \quad (3)$$

As seen in Fig. 8, the effectiveness of the diffuser decreases slightly with increasing blowing fraction.

Total drag reduction

The total drag reduction—or better, thrust enhancement—due to micro-blowing is obtained directly from the force balance measurement and the pressure tare calibration. The total drag reduction provides a measure of the benefit derived by reducing skin friction while at the same time increasing aerodynamic blockage and hence reducing pressure recovery in the aft portion of the strut. In Fig. 9, the normalized drag coefficients are plotted as a function of reduced blowing fraction. Values greater than unity mean that the net thrust of the treated airfoil is greater than the net thrust of the airfoil at zero blowing. In all cases, net positive blowing is better than zero blowing. Another important comparison is shown in Fig. 10. The drag coefficients from treated struts at various blowing fractions are compared with the baseline, solid-plate values, at three different Mach numbers. The range bands give a good indication of scatter in the force balance measurements. Considering the mean values however, thrust is increased (or drag is effectively reduced) relative to the solid-plate thrust, provided that the reduced blowing fraction level is sufficiently high (e.g., $F^+ \geq 0.5$ for $M = 0.7$).

Wake profiles

Comparison of wake survey data obtained from the traversing total pressure probe at various levels of blowing and for the baseline solid-plate case are shown in Fig. 11. Wake parameters are shown in Table 2. Note that these results are qualitatively consistent with the analytical results for the Blasius flow in zero-pressure-gradient shown in Table 1. The micro-blowing increases the wake thicknesses and shape factors. The shape factor appears to approach 1.53 asymptotically. Note that the shape factor at the MBT-treated strut in the zero-blowing limit is lower than that of the solid-plate. At low reduced blowing fractions, the MBT treated struts have higher mass-averaged total pressure

than does the solid-plate strut. Although theory suggests that the loss production in the boundary layer is reduced by micro-blowing, the mass-averaged total pressure is reduced as blowing air is increased because of the deposition of the low total pressure blowing air.

Discussion

The functional dependence of C_f^* with F^+ is shown in Fig. 6 and is in excellent agreement with the data compiled by Hefner and Bushnell⁶ from a number of sources, which spans a wide-range of Mach numbers and conditions. The agreement suggests that the functional dependence holds independent of Reynolds and Mach numbers, pressure gradient, and blowing strategy (e.g., hole size or porosity distribution). However, as noted in earlier work by Hwang¹, the selection of efficient MBT skin is by no means arbitrary. Indeed, the micro-blowing skin was chosen to accommodate the blowing air effusion that effects the C_f^* vs F^+ behavior (i.e., skin friction reduction) while also assuring that $C_{f,0} = C_{f,s}$.

The functional dependence of the ratio of the total drag of the MBT-treated strut with finite blowing to the total drag of the MBT-treated strut with zero-blowing ($C_D/C_{D,0}$) on the reduced blowing fraction is shown in Fig. 9. The normalized total drag is effectively reduced by micro-blowing at all levels; further, as shown in Fig. 10, the blowing effectively reduces the total drag of the MBT-treated strut below that of the baseline (solid-plate) strut, provided that the reduced blowing fraction, F^+ , is sufficiently high. The break-even F^+ depends on the Mach number. It is noted, however, that the thickness-to-chord ratio (W/L) scales the impact of the increased pressure drag (or in the present case, reduced pressure thrust) associated with the lack of pressure recovery due to aerodynamic blockage (cf. Eqn 1 and Fig. 4). The attained total drag reduction is in general dependent on the thickness-to-chord ratio or the trade between skin friction benefit and pressure drag penalty.

As expected, the addition of the micro-blowing air at low total pressure increases aerodynamic blockage and, in all cases, results in lower diffuser c_p (see Fig. 7).

The diffuser effectiveness was reduced very slightly by the MBT treatment (Fig 8). This last finding runs contrary to the slight increase in diffuser effectiveness anticipated by the authors and to the notion that MBT can be used to increase the effectiveness of diffusing sections. It is also noted that the deeper, thicker wakes introduced by the MBT-treatment could lead to higher mixing losses; hence, in some applications, although the entropy production in the boundary layer is reduced, the overall entropy production associated with the boundary-layer dissipation and wake mixing could be

increased. Perhaps an accelerating, high-speed section, especially one in which the effusion cooling is required, might be a fruitful internal flow application of the micro-blowing technique.

Summary

The experimental data reported herein indicate that the MBT technique effectively decreases skin friction in strong adverse pressure gradients. Consistent with a Blasius solution for transpired flows, wake surveys downstream of the micro-blown strut showed that the effused blowing air increases the boundary layer displacement and momentum thicknesses and shape factor. In terms of diffuser performance, the increased aerodynamic blockage associated with the blowing air results in lower diffuser static pressure rise coefficient and effectiveness. For external flows, the reduced pressure recovery results in increased pressure drag. The trade between increased pressure drag due to aerodynamic blockage and reduced skin friction hinges on the thickness-to-chord ratio of the airfoil. For the long, narrow strut tested herein, drag of the MBT-treated strut with finite blowing was effectively lower than the drag of the treated strut in the zero blowing limit. Further, the total drag of the MBT-treated strut was effectively reduced below the total drag of the baseline (solid-plate) strut, provided that the reduced blowing fractions were sufficiently high.

Acknowledgements

The authors thank Dr. Eric R. McFarland of NASA Glenn Research Center for supporting this work with panel code calculations, Mr. Charles A. Herrmann for

engineering design work, and Ms. Gwynn A. Severt, Mr. Carlos R. Gomez, and Mr. Scott R. Panko for facility set-up, operation, and testing.

References

- ¹Hwang, D. P., "A Proof of Concept Experiment for Reducing Skin Friction by using a Micro-Blowing Technique," NASA TM-107315, Jan., 1997.
- ²Tillman, T. G., "Drag Reduction on a Large-Scale Nacelle using Micro-Porous Blowing," R97-4.910.0001, NASA LeRC LET, Task 50, United Technologies, Dec., 1997.
- ³Hwang, D. P. and Biesiadny, T. J., "Experimental Evaluation of the Penalty Associated with Micro-Blowing for Reducing Skin Friction," NASA TM-113174, Dec., 1997.
- ⁴Schlichting, H., *Boundary-Layer Theory*, McGraw-Hill, Inc., USA, 1979, pp. 389-391.
- ⁵White, F. M., *Viscous Fluid Flow*, McGraw-Hill, Inc., USA, 1974, pp. 675-678.
- ⁶Hefner, J. N. and Bushnell, D. M., "Viscous Drag Reduction via Surface Mass Injection," ed., Bushnell, D. M. and Hefner, J. N., *Viscous Drag Reduction in Boundary Layers*, AIAA Inc., USA, 1990, pp. 457-476.
- ⁷Shapiro, A. H., *Compressible Fluid Flow*, Ronald Press, USA, 1953, pp. 151-152.

Table 1. Parameters from Blasius solution of zero-pressure-gradient flow with transpiration ($2\sqrt{Re_x} = 350$).

F	δ_0^\dagger	δ_1	δ_2	H	f''	δ_1^*	δ_2^*	ω^*	C_f^*	F^*	$C_f^* + F^*$
-0.001	4.2	1.30	0.543	2.38	0.533	0.75	0.81	1.55	1.604	-0.79	0.81
0	5.0	1.72	0.666	2.59	0.332	1.0	1.0	1.0	1.0	--	1.0
0.001	6.2	2.51	0.840	2.99	0.157	1.46	1.26	0.61	0.473	0.79	1.26

[†] δ_0, δ_1 , and δ_2 are reported here in terms of the Blasius similarity variable.

Table 2. Normalized wake survey parameters 1/3-chord downstream of strut (Mach 0.7).

F^*	$2^* \delta_0 / L$	δ_1^*	δ_2^*	H	\dot{m} / ft	$\bar{P}_0 / p_{0,\infty}$	$\bar{P}_0 / p_{0,\infty}$
solid	0.104	0.792	0.768	1.44	0.9918	0.9698	0.9697
0.0	0.138	1.00	1.0	1.40	0.9943	0.9726	0.9725
0.25	0.158	1.10	1.04	1.49	0.9894	0.9711	0.9709
0.50	0.151	1.17	1.08	1.52	0.9887	0.9688	0.9686
0.75	0.139	1.27	1.16	1.53	0.9890	0.9630	0.9627

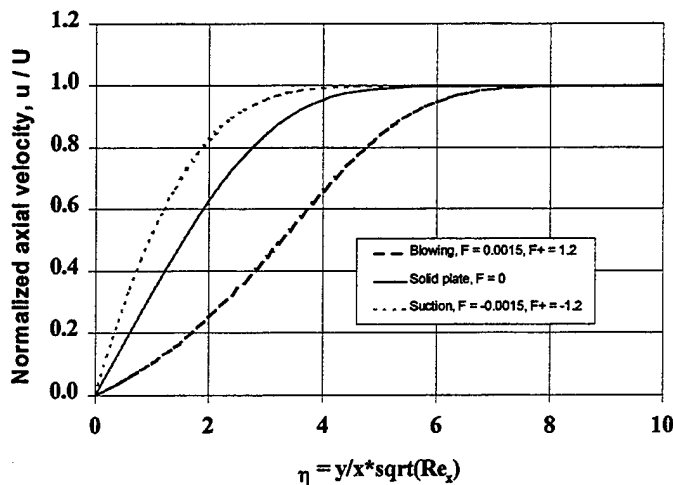


Figure 1. Normalized axial velocity profiles from Blasius solution of transpired flows.

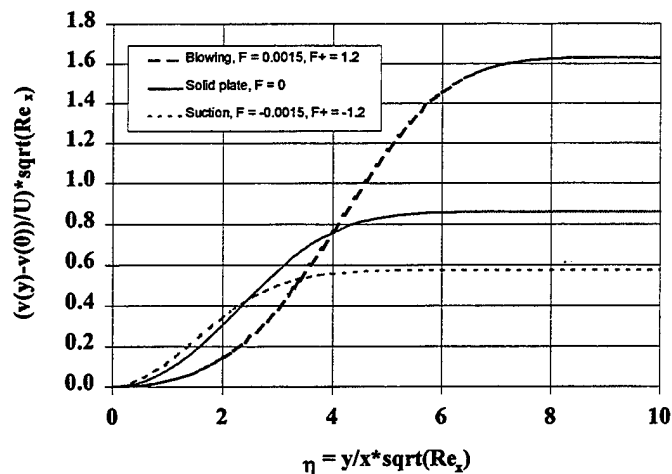


Figure 2. Normalized transverse relative velocity profiles from Blasius solution of transpired flows.

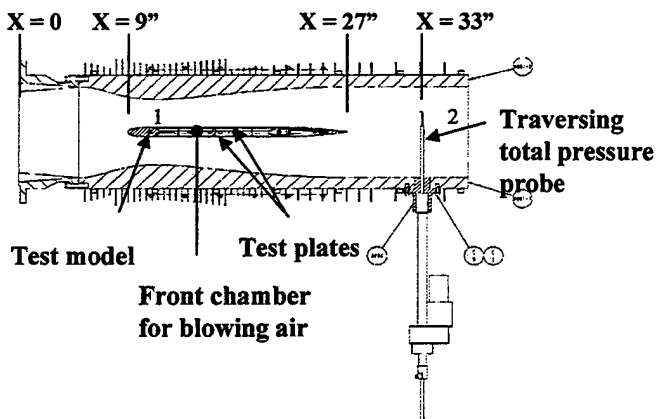


Figure 3. Schematic diagram of 2-D diffuser (top view) showing strut test model and traversing total pressure rake for wake surveys.

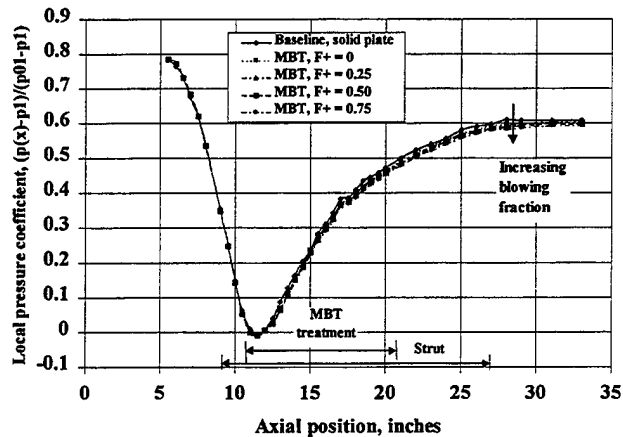


Figure 4. Local pressure coefficient at mid-height along sidewall as a function of axial position at Mach 0.7 throat conditions, showing the impact of MBT treatment at various blowing levels.

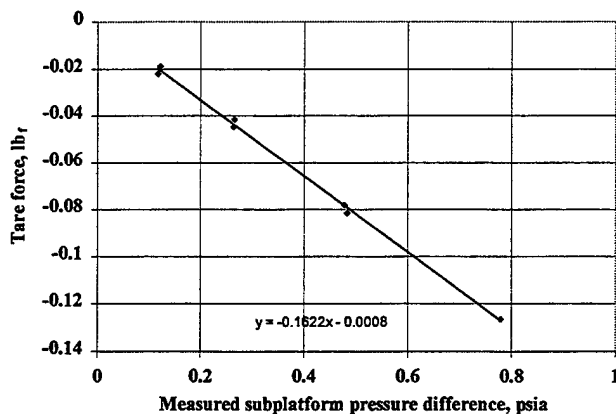


Figure 5. Calibration curve for tare force to account for pressure loading on mounting stand.

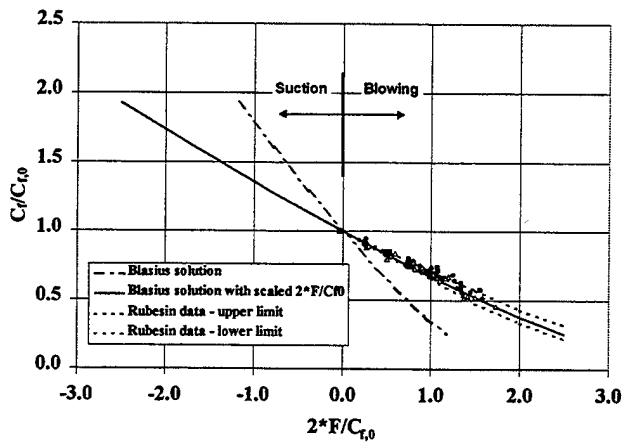


Figure 6. Normalized integral skin friction coefficient as a function of reduced blowing fraction, showing data from present experiment at all Mach numbers (symbols), dashed curves that bound the Rubesin data as reported in Ref. 6, and curves of Blasius solution.

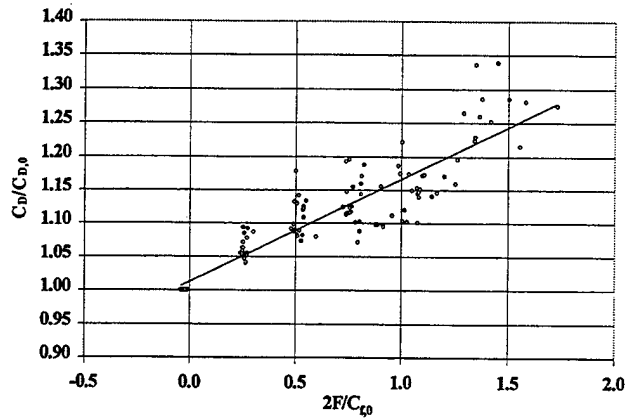


Figure 9. Normalized drag coefficient as function of reduced blowing fraction.

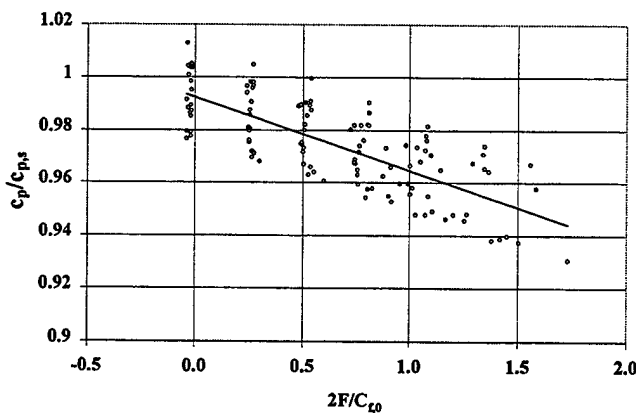


Figure 7. Diffuser static pressure rise coefficient normalized by baseline (solid-plate) value as a function of reduced blowing fraction.

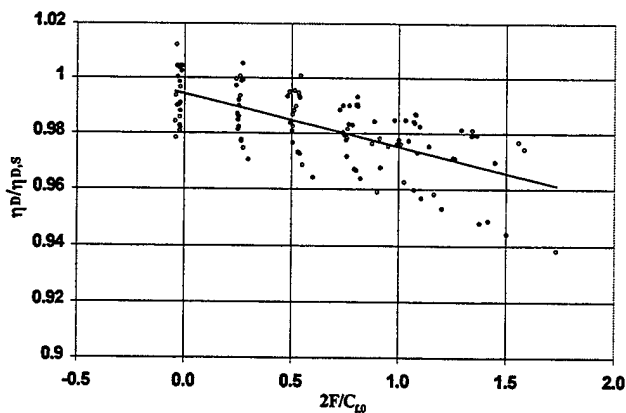


Figure 8. Diffuser effectiveness normalized by baseline (solid-plate) value as a function of reduced blowing fraction.

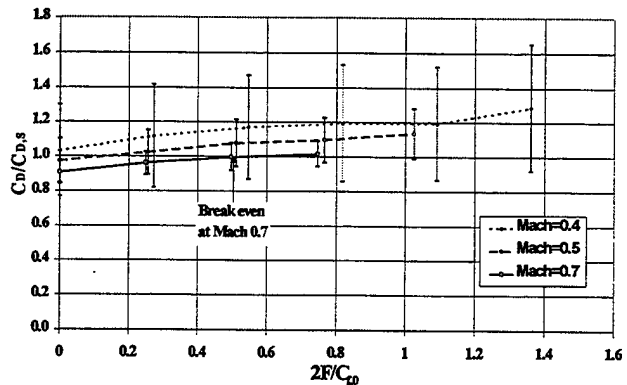


Figure 10. Drag coefficient normalized by baseline (solid-plate) value as a function of reduced blowing fraction.

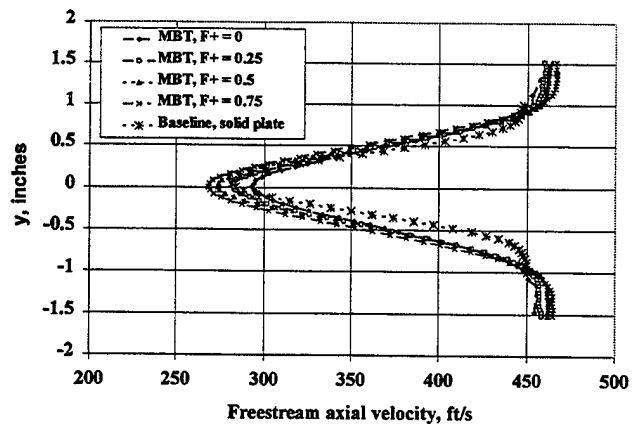


Figure 11. Velocity from total pressure traverse at 1/3-chord (7.5 strut-widths) downstream of strut, showing impact of various blowing levels.

REPORT DOCUMENTATION PAGE

Form Approved
OMB No. 0704-0188

Public reporting burden for this collection of information is estimated to average 1 hour per response, including the time for reviewing instructions, searching existing data sources, gathering and maintaining the data needed, and completing and reviewing the collection of information. Send comments regarding this burden estimate or any other aspect of this collection of information, including suggestions for reducing this burden, to Washington Headquarters Services, Directorate for Information Operations and Reports, 1215 Jefferson Davis Highway, Suite 1204, Arlington, VA 22202-4302, and to the Office of Management and Budget, Paperwork Reduction Project (0704-0188), Washington, DC 20503.

1. AGENCY USE ONLY (Leave blank)		2. REPORT DATE January 2001	3. REPORT TYPE AND DATES COVERED Technical Memorandum	
4. TITLE AND SUBTITLE Effectiveness of Micro-Blowing Technique in Adverse Pressure Gradients			5. FUNDING NUMBERS WU-708-28-13-00 1L162211A47A	
6. AUTHOR(S) Gerard E. Welch, Louis M. Larosiliere, Danny P. Hwang, and Jerry R. Wood				
7. PERFORMING ORGANIZATION NAME(S) AND ADDRESS(ES) National Aeronautics and Space Administration John H. Glenn Research Center Cleveland, Ohio 44135-3191 and U.S. Army Research Laboratory Cleveland, Ohio 44135-3191			8. PERFORMING ORGANIZATION REPORT NUMBER E-12617	
9. SPONSORING/MONITORING AGENCY NAME(S) AND ADDRESS(ES) National Aeronautics and Space Administration Washington, DC 20546-0001 and U.S. Army Research Laboratory Adelphi, Maryland 20783-1145			10. SPONSORING/MONITORING AGENCY REPORT NUMBER NASA TM-2001-210690 ARL-TR-2382 AIAA-2001-1012	
11. SUPPLEMENTARY NOTES Prepared for the 39th Aerospace Sciences Meeting and Exhibit sponsored by the American Institute of Aeronautics and Astronautics, Reno, Nevada, January 8-11, 2001. Gerard E. Welch and Louis M. Larosiliere, U.S. Army Research Laboratory, Glenn Research Center, Cleveland, Ohio; Danny P. Hwang and Jerry R. Wood, NASA Glenn Research Center. Responsible person, Gerard E. Welch, organization code 5810, 216-433-8003.				
12a. DISTRIBUTION/AVAILABILITY STATEMENT Unclassified - Unlimited Subject Category: 07 Available electronically at http://gltrs.grc.nasa.gov/GLTRS This publication is available from the NASA Center for AeroSpace Information, 301-621-0390.			12b. DISTRIBUTION CODE Distribution: Nonstandard	
13. ABSTRACT (Maximum 200 words) The impact of the micro-blowing technique (MBT) on the skin friction and total drag of a strut in a turbulent, strong adverse-pressure-gradient flow is assessed experimentally over a range of subsonic Mach numbers ($0.3 < M < 0.7$) and reduced blowing fractions ($0 \leq 2F/C_{f0} \leq 1.75$). The MBT-treated strut is situated along the centerline of a symmetric 2-D diffuser with a static pressure rise coefficient of 0.6. In agreement with presented theory and earlier experiments in zero-pressure-gradient flows, the effusion of blowing air reduces skin friction significantly (e.g., by 60% at reduced blowing fractions near 1.75). The total drag of the treated strut with blowing is significantly lower than that of the treated strut in the limit of zero-blowing; further, the total drag is reduced below that of the baseline (solid-plate) strut, provided that the reduced blowing fractions are sufficiently high. The micro-blowing air is, however, deficient in streamwise momentum and the blowing leads to increased boundary-layer and wake thicknesses and shape factors. Diffuser performance metrics and wake surveys are used to discuss the impact of various levels of micro-blowing on the aerodynamic blockage and loss.				
14. SUBJECT TERMS Skin friction; Drag reduction; Micro-blowing technique			15. NUMBER OF PAGES 14	
			16. PRICE CODE A03	
17. SECURITY CLASSIFICATION OF REPORT Unclassified	18. SECURITY CLASSIFICATION OF THIS PAGE Unclassified	19. SECURITY CLASSIFICATION OF ABSTRACT Unclassified	20. LIMITATION OF ABSTRACT	